Climate Dynamics
https://doi.org/10.1007/s00382-021-06120-0

Prediction of extreme events in precipitation and temperature over CONUS during boreal summer in the UFS coupled model

V. Krishnamurthy[1] · **Cristiana Stan**[2]

Received: 10 August 2021 / Accepted: 22 December 2021

Abstract
The predictions of extreme events by the Unified Forecast System (UFS) Coupled Model Prototype 5 of the National Centers for Environmental Prediction over the contiguous United States during boreal summer are assessed. The extreme events in precipitation and daily maximum and minimum surface air temperature in weeks 1–4 predictions are analyzed in the deterministic retrospective forecasts of UFS during 2011–2017. The spatial structures of the extreme events in precipitation are reasonably well predicted but with higher values. Although the predictions of the temperature are closer to observation over central and eastern parts of the US, the model fails to generate the extreme events over large western regions. There is no appreciable growth of forecast errors of extreme events during weeks 1–4. While the spatial correlation of the number of extreme events between the forecasts and observation is very low for precipitation and temperature, the correlation of the temperature per event is very high. The model is able to better predict the observed location and magnitude of temperature events whenever it can generate such events. The number of precipitation events in the forecasts is higher than in the observation but with less accuracy in location and magnitude. The influence of slowly varying modes related to El Niño-Southern Oscillation (ENSO), intraseasonal oscillation (ISO) and warming trend of the ocean on the extreme events are also studied. All three modes have enhancing influence on precipitation while only the ENSO mode enhances the maximum temperature events. The minimum temperature events are enhanced by ENSO and ISO but diminished by the warming trend.

Keywords Extreme events · Unified Forecast System · Contiguous United States · Prediction

1 Introduction

Changes in the mean climate observed since the mid-20th century are likely responsible for the increase in the number of heavy precipitation events (e.g., 95th percentile) and warming of extreme daily and minimum temperatures at the continental scale including the North America (Seneviratne et al. 2012). Projected precipitation extremes suggest a strong increase in extreme precipitation over the southern and central US (Zhang et al. 2008) during winter and in the southeastern US during summer (Zhu and Stan 2015). Projections of changes in temperature extremes on weather time scales (i.e., daily mean, maximum and minimum temperatures) are very consistent across climate models (Seneviratne et al. 2012). These extreme events and their cumulative effects (i.e., heat waves, cold spells, floods, droughts) have daunting socio-economic costs (Vitart and Robertson 2018). Therefore, prediction of extremes of atmospheric weather events, such as precipitation and temperature, by extended range forecasting systems become imperative to better prepare for and mitigate extreme weather hazards.

The forecast skill of extremes poses scientific challenges related to the nature and source of predictability of the event. Extremes of atmospheric weather are not caused by variations in a single atmospheric variable, but generally result from specific conditions or states determined by the climate modes of variability (e.g., Stan et al. 2017). These modes affect the large-scale environment, which in turn influences the extremes. For example, during the boreal winter, the frequency of extreme cold temperatures over the Pacific Northwest and southwestern US increases when the Madden-Julian Oscillation (MJO) convective anomalies are

✉ V. Krishnamurthy
vkrishna@gmu.edu

[1] Center for Ocean-Land-Atmosphere Studies, George Mason University, Fairfax, VA, USA

[2] Department of Atmospheric, Oceanic and Earth Sciences, George Mason University, Fairfax, VA, USA

Published online: 10 January 2022

located in the Indian Ocean (Vecchi and Bond 2004). The frequency of nor'easters in the northeastern US tends to be higher during MJO episodes with strong convective activity during phase 7 and 8 (Klotzbach et al. 2016). The frequency of extreme rainfall events over the Pacific Northwest and the southeastern US increases when the MJO convective anomalies are active (Jones 2000) and these extreme events become more predictable (Jones et al. 2011; Huang et al. 2021). During the boreal summer, the US precipitation variability on subseasonal-to-seasonal (S2S) time scale can also be affected by MJO (Zhou et al. 2012) and other modes of climate variability operating on intraseasonal to interannual time scales as well as long-term trends (Krishnamurthy et al. 2021). During the boreal summer, weather extremes in the US are mostly attributed to local land-atmosphere feedbacks (Koster et al. 2004; Clark et al. 2006) whereas the relationship between extremes and regional climate modes of variability is less understood.

Studies evaluating the forecast skill of extreme events on extended range time scales are scarce. Over North America, the current generation of S2S models (Vitart et al. 2016) show promising skill for some case studies of extreme temperature events (Vitart and Robertson 2018) and less skill for flooding events (Lin et al. 2019; Stan and Lin 2019). Lin et al. (2019) found that most models predict the above-normal precipitation a few weeks in advance, but the magnitude of the anomaly is underestimated. A study of the Coupled Model Intercomparison Project Phase 6 (CMIP6) coupled models showed that the estimation of the intensity of extreme precipitation over the US varies across of all the models (Srivastava et al. 2020).

The objective of this study is to understand the extreme events in precipitation and 2 m temperature over the contiguous United States (CONUS) during the boreal summer and to assess the predictability of such events by a coupled model at subseasonal time scale. For this purpose, the retrospective forecasts of the coupled model from the National Centers for Environmental Predictions (NCEP) of the National Oceanic and Atmospheric Administration (NOAA) are used for the boreal summer of 2011–2017. The model's ability to predict the extreme events in precipitation, daily maximum 2 m temperature and daily minimum 2 m temperature over the CONUS in weeks 1–4 will be studied. A quantitative assessment of the predictability will be carried out by examining the error growth and spatial correlation between the forecasts and observations. Further, the influence of the leading modes of slow large-scale variability on the extreme events will also be investigated.

A description of the coupled model and its retrospective forecasts, observed data and the reanalysis data used in this study is given in Sect. 2. In Sect. 3, the extreme events in precipitation and 2 m temperature in the observations and their prediction by the model are described. An assessment of the predictability of the extreme events by the model is provided in Sect. 4. The association of the leading modes of variability with the extreme events is discussed in Sect. 5. The summary and conclusion are given in Sect. 6.

2 Model and data

2.1 Model

The Unified Forecast System (UFS) Coupled Model Prototype 5, developed by the NCEP, is the model used in this study (Krishnamurthy et al. 2021). This coupled model version of the UFS consists of an atmospheric component (FV3GFS) with C384 (~28 km) resolution, an oceanic component (GDDL MOM6 model, Adcroft et al. 2019) and a sea-ice component (Los Alamos CICE6 model) with tripolar 0.25° global grid. For the period April 2011–December 2017, 35-day long retrospective forecasts were generated by the NCEP starting from first and fifteenth of each month. The Climate Forecast System Reanalysis data were used to initialize the atmospheric model while the Climate Prediction Center (CPC) Hybrid Global Ocean Data Assimilation System provided the initial conditions for the ocean model. The sea-ice model was initialized by the CPC ice analysis. Because this study is concerned with the boreal summer, daily values of various variables of the reforecasts are analyzed only during June–September (JJAS) of 2011–2017. This analysis period consists of 56 deterministic reforecasts corresponding to the 28 months, each with two initial conditions. The model used in this study is a modified version of the model used in a recent study (Krishnamurthy et al. 2021) that investigated the sources of predictability at intraseasonal time scale over CONUS. The modifications involve the sea-ice model and its initial condition, atmospheric physics driver, and ocean-atmosphere coupling. The previous study (Krishnamurthy et al. 2021) has discussed the modes of variability in circulation, precipitation and average 2 m temperature over CONUS in the model's retrospective forecasts and compared them with the observation. Further, the study assessed the predictability of the modes in the UFS at weeks 1–4 range. The rest of the present paper will refer to the retrospective forecasts simply as forecasts for convenience and brevity.

2.2 Data

The daily maximum and minimum temperature at 2 m on a 0.5° × 0.5° grid over CONUS were obtained from the CPC analysis for the period 2011–2017. For brevity, these temperatures will be referred to as simply maximum temperature and minimum temperature, hereafter. The CPC unified (CPCU) gauge-based analysis of global precipitation

(Xie et al. 2010) provided the daily precipitation on a 0.5° × 0.5° grid for the period 2011–2017. From the European Centre for Medium-Range Weather Forecasts Reanalysis—Interim (ERAI, Dee et al. 2011) data set, the zonal velocity (u) and meridional velocity (v) at 850 hPa on T255 horizontal grid (~0.703° resolution) were obtained for the period 1979–2017.

3 Extreme events in precipitation and 2 m temperature

The definition of extreme events is quite varied and chosen on the basis of the suitability to the temporal and spatial structures of the domain, as described in the reviews of extreme precipitation and temperature over North America (Grotjahn et al. 2016; Barlow et al. 2019). These reviews have indicated that the most commonly used measure is based on exceeding a threshold of fixed value or frequency of occurrence such as a quantile. The selection of extreme events in this study is based on the percentile of the variable at each grid point at any given time during the period of JJAS 2011–2017. The threshold for extreme events in precipitation is the 95th percentile of the daily values of wet days (i.e., when the daily mean value is greater than zero) during JJAS 2011–2017, in a manner similar to several earlier studies on CONUS (e.g., Singh et al. 2013). An event above the threshold value on a particular day is counted as one extreme event. For the maximum temperature, the extreme events are above the threshold of 95th percentile of all the days during JJAS 2011–2017. The extreme events of the minimum temperature are those below the threshold of 5th percentile of all the days of JJAS 2011–2017. A systematic examination of the events occurring at various percentile ranges was carried out before selecting the threshold values of extreme events used in this study. The analysis will also consist of brief comparisons, where appropriate, with extreme events based on 99th percentile for precipitation and maximum temperature and 1st percentile for minimum temperature. The 99th, 95th, 5th and 1st percentiles will be abbreviated as 99P, 95P, 5P and 1P, respectively, hereafter.

The 95P threshold values for precipitation and maximum temperature and 5P values for minimum temperature are shown in Fig. 1 for observations and model forecasts.

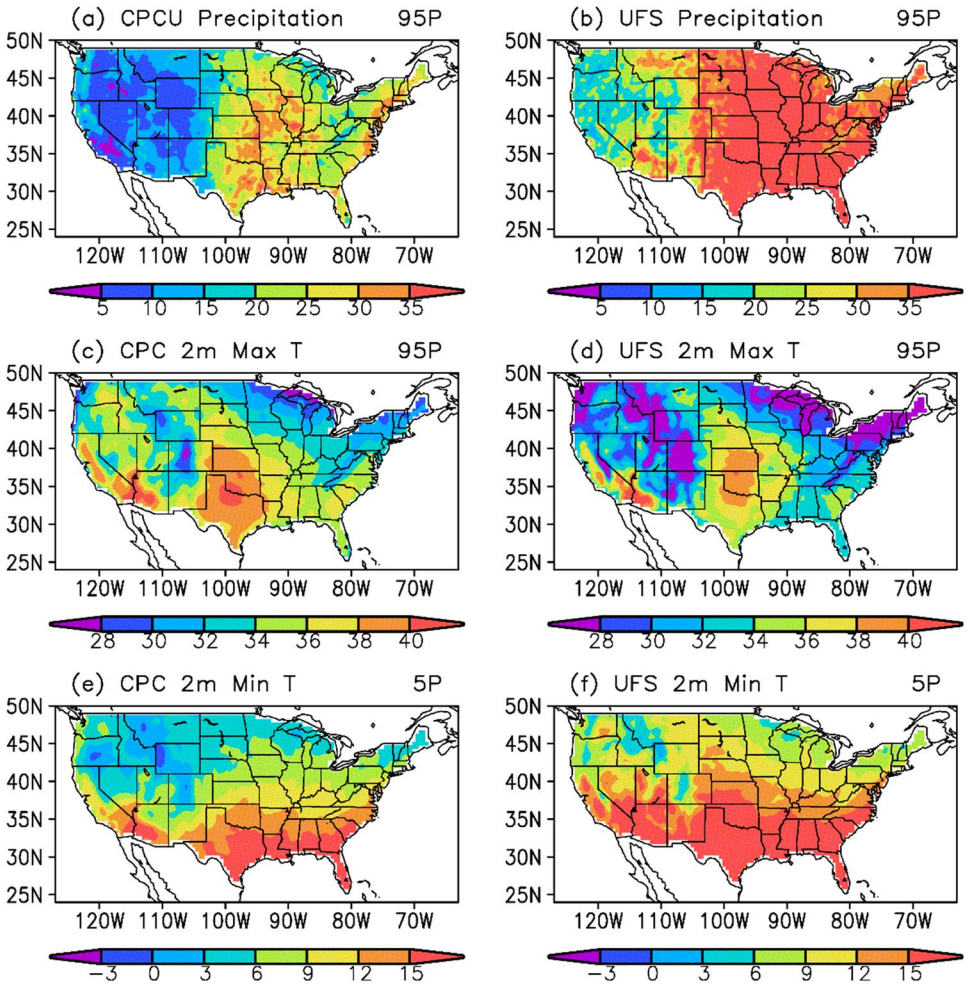

Fig. 1 95th percentile of precipitation (mm day^{-1}) in **a** CPCU observation and **b** UFS forecasts, 95th percentile of daily maximum 2 m temperature (°C) in **c** CPC observation and **d** UFS forecasts and 5th percentile of daily minimum 2 m temperature (°C) in **e** CPC observation and **f** UFS forecasts for the period JJAS 2011–2017 over CONUS. The percentile values are based on the values of all the days of JJAS 2011–2017. In the model, all the forecasts initiated from 1st and 15th of each month during JJAS 2011–2017 are used

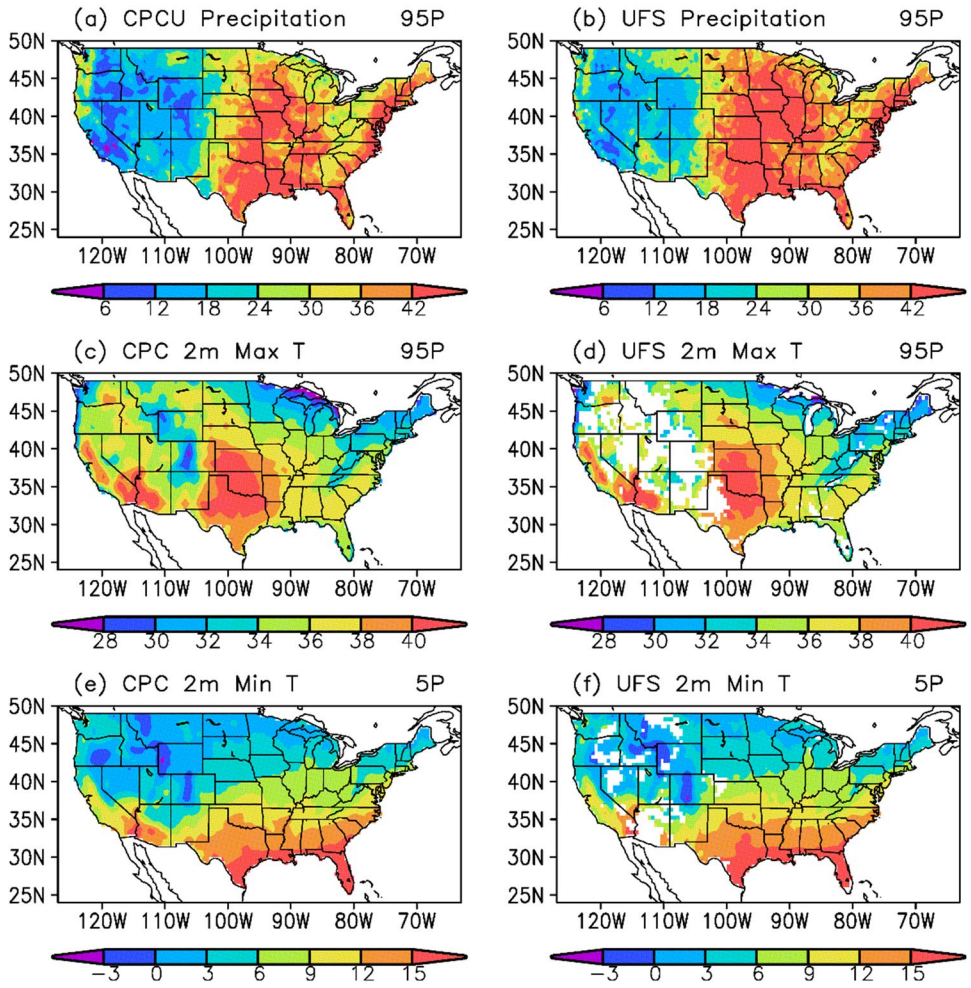

Fig. 2 Composites of precipitation (mm day^{-1}) in **a** CPCU observation and **b** UFS forecasts exceeding the 95P of observation, composites of daily maximum 2 m temperature (°C) in **c** CPC observation and **d** UFS forecasts above the 95P of observation and composites of daily minimum 2 m temperature (°C) in **e** CPC observation and **f** UFS forecasts below the 5P of observation for the period JJAS 2011–2017 over CONUS. All the forecasts initiated from 1st and 15th of each month during JJAS 2011–2017 are used in the composites. The composites are averages over the entire period. The unshaded white regions over CONUS indicate that the extreme events did not occur at those grid points

The 95P value of observed CPCU precipitation (Fig. 1a) is lower in the West in the range of 5–20 mm day^{-1} while the eastern half of the US is in the higher range of 20–40 mm day^{-1}. The Midwest, some of the southern states and a part of the east coast are in the highest range, reflecting perhaps higher convective or storm activities in those regions. In the model forecasts (Fig. 1b), the 95P of precipitation is generally higher than the observed values (Fig. 1a) over the entire CONUS. The forecasts also show a lower range (15–25 mm day^{-1}) in the western states while the Midwest and most of the eastern part are in the range of 30–40 mm day^{-1}.

The 95P of maximum temperature in the CPC observation (Fig. 1c) shows the highest values (36–40 °C) in several southern and southwest states while lowest values (28–34 °C) are seen in the northeastern region, Midwest and some western states. The corresponding threshold in the model forecasts (Fig. 1d) is generally lower by about 2–4 °C over the CONUS. The maximum temperature is in the range of 28–34 °C except for a part of the central US and the Southwest where it is about 34–40 °C. The 5P of minimum temperature in the observation (Fig. 1e) shows lower values over most of the northern part in the range of − 3–9 °C while the southern part is about 9–18 °C. However, the model forecasts have 5P values higher than the observation over the entire CONUS, differing generally by about 3–6 °C over most regions.

The 99P values of precipitation and temperature in observations and model forecasts are shown in Fig. S1 in the supplementary material. The spatial structures of 99P values (Fig. S1) are similar to those of 95P values (Fig. 1) but with higher threshold values. The 99P of precipitation in the observation (Fig. S1a) is similar to the 95P but with higher values. The 99P values of precipitation are generally about 1.7–2.0 times the 95P values in both observation and model forecasts. The 99P in the model forecasts (Fig. S1b) has a better correspondence with the observation compared to the case of 95P. The maximum temperature at 99P is about 2 °C higher than the 95P values. The highest values at 99P are seen over a wider region covering Texas and neighboring states in observation while they are shifted to the north in model forecasts (Fig. S1c, d). The 1P values of minimum temperature are generally about 2–3 °C lower than the 5P values. The 1P values of model forecasts are higher than the observation over most of the CONUS. These comparisons

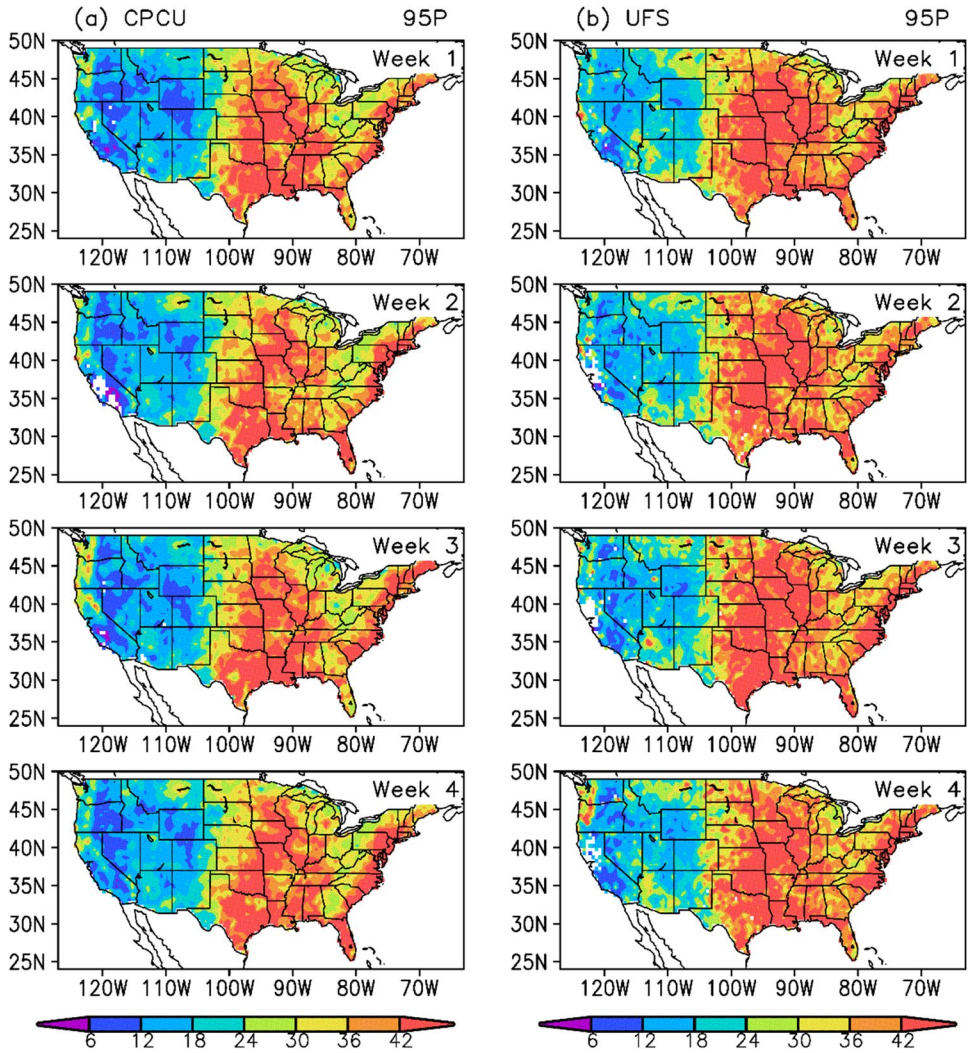

Fig. 3 Weekly composites of precipitation per event (mm day^{-1}) above 95P of CPCU in **a** CPCU observations and **b** UFS forecasts. The first 4 weeks of the forecasts initiated from 1st and 15th of each month during JJAS 2011–2017 are used in the composites. The unshaded white regions over CONUS indicate that the extreme events did not occur at those grid points

between the climatology of extreme events in observations and forecasts show that the model has systematic biases in reproducing the pattern and magnitude of precipitation and temperature extremes. Eliminating these biases is beyond the scope of this study, and the definition of extreme events in the model will be based on the same threshold as in observation.

To examine the model's ability to predict the end tail of observed precipitation and temperature distributions, the composites of precipitation and temperature that rank above the extreme percentile threshold values were analyzed. The 95P (99P) composites of precipitation and maximum temperature were constructed by first adding the values of events in the observations and model forecasts, separately, above the 95P (99P) threshold values in observation for the period JJAS 2011–2017 and then dividing by the respective number of events. Similarly, the 5P (1P) composites of minimum temperature were constructed when the temperature is below the 5P (1P) threshold value in observation. Since model's forecasts are meant to predict what will be observed, it is only appropriate to select the extreme events in the forecasts that cross the threshold in observations.

The 95P composite of precipitation in observation (Fig. 2a) shows most of the western part below 24 mm day^{-1} while a large part of the Midwest and the eastern US is above 40 mm day^{-1}. Although the model forecasts are similar to the observed pattern, the extreme precipitation is higher with a large part over the Midwest and East exceeding 42 mm day^{-1}. The 99P composites of precipitation in observation (Fig. S2a) and forecasts (Fig. S2b) have spatial structure similar to the 95P composites (Fig. 2) but with values that are about 1.5 times higher over the entire CONUS. The 99P composites of forecasts (Fig. S2b) are also higher than the observations (Fig. S2a) with values exceeding 63 mm day^{-1} over the Midwest and East but fail to generate the observed extreme events over some parts of Texas and California.

For the maximum temperature, the 95P composite of observations (Fig. 2c) consists of higher values (36–40 °C) over southern and Southwest states while lower values (28–34 °C) are seen in northern and western states. The

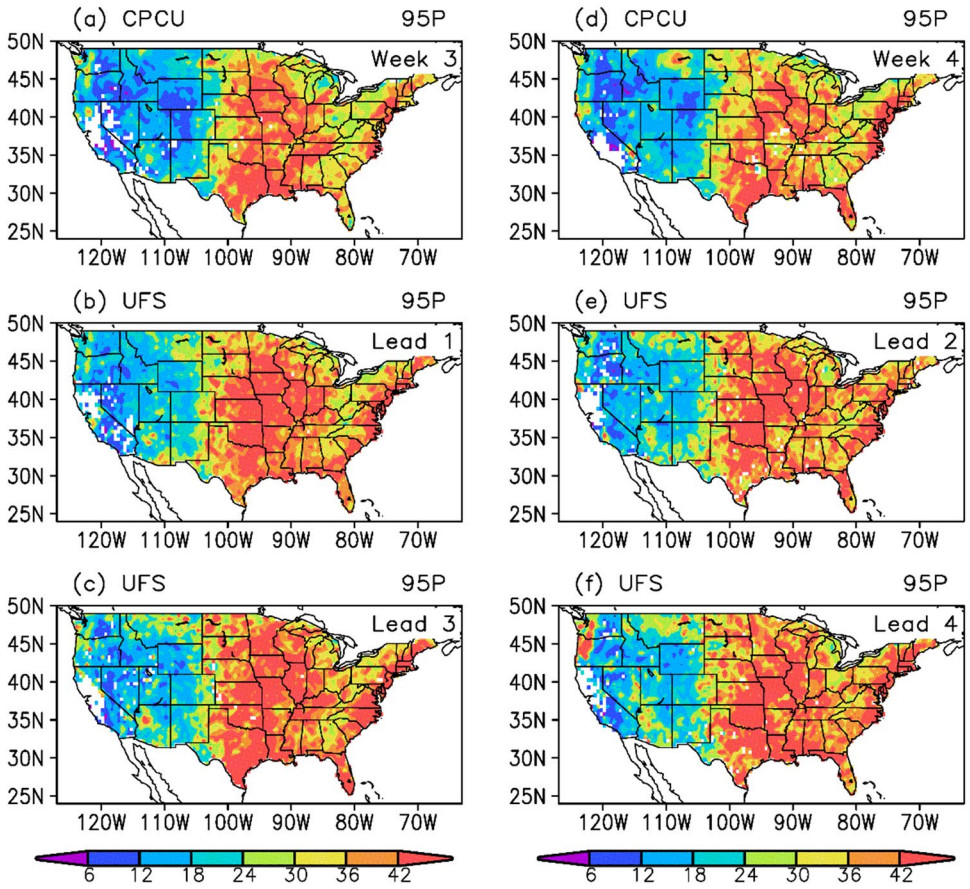

Fig. 4 Weekly composites of precipitation per event (mm day^{-1}) above 95P of CPCU in **a** CPCU observations for week 3, and corresponding UFS forecasts with **b** lead of 1 week and **c** lead of 3 weeks. Weekly composites of **d** CPCU observations for week 4, and corresponding UFS forecasts with **e** lead of 2 week and **f** lead of 4 weeks. The first 4 weeks of the forecasts initiated from 1st and 15th of each month during JJAS 2011–2017 are used in the composites. The unshaded white regions over CONUS indicate that the extreme events did not occur at those grid points

forecasts (Fig. 2d) are close to the observed values in most of region to the east of 105°W while failing to generate the extreme events over most of the region to the west. However, the model captures the observed values in certain small parts of Southwest and northern states. The 99P composite of maximum temperature in the observations (Fig. S2c) shows the highest values (above 40 °C) over Texas and neighboring states and a part of the Southwest while the lowest values (below 34 °C) are seen in some northern and western states. The 99P composite reveals that the forecasts (Fig. S2d) generate the observed pattern and values (Fig. S2c) over only a limited region confined to the Midwest and Southwest while missing in the rest of the CONUS.

In the 5P composite of minimum temperature in the observations (Fig. 2e), higher values above 12 °C cover most of the southern states and the Southwest while the coldest states are in the West and the northern part. The corresponding composite in the forecasts (Fig. 2f) shows temperatures higher by roughly 3 °C compared to the observations (Fig. 2e) over most of the CONUS. The highest values (above 15 °C) cover a larger area over most of the South and a part of the Midwest. The forecasts, however, fail to generate the observed extreme events over states in the West and South. In the 1P composite of minimum temperature in the observations (Fig. S2e), most of the northern part is below 3 °C and reaches below − 3 °C over Wyoming and Montana. The 1P composite of the forecasts (Fig. S2f) shows that the model is not able to generate the extreme events over a large region to the west of 100°W. However, over the rest of CONUS, the extreme events of the forecasts are close to the observations in both pattern and magnitude.

4 Prediction of extreme events

Since the objective of this study is to assess the predictability of the extreme events by the model in the subseasonal time scale, the weekly predictions of precipitation and 2 m temperature are examined. For this purpose, the weekly composites of extreme events for each of the first 4 weeks of the forecasts initiated from first and fifteenth of each month during JJAS 2011–2017 are constructed. The weekly composites are expressed as precipitation or temperature per event after dividing the sum of the extreme values by the number of events during the period. The corresponding weekly composites are also constructed for the observations. The number of extreme events in these composites at any grid point may differ between observation and forecasts. The weekly composites of both the forecasts

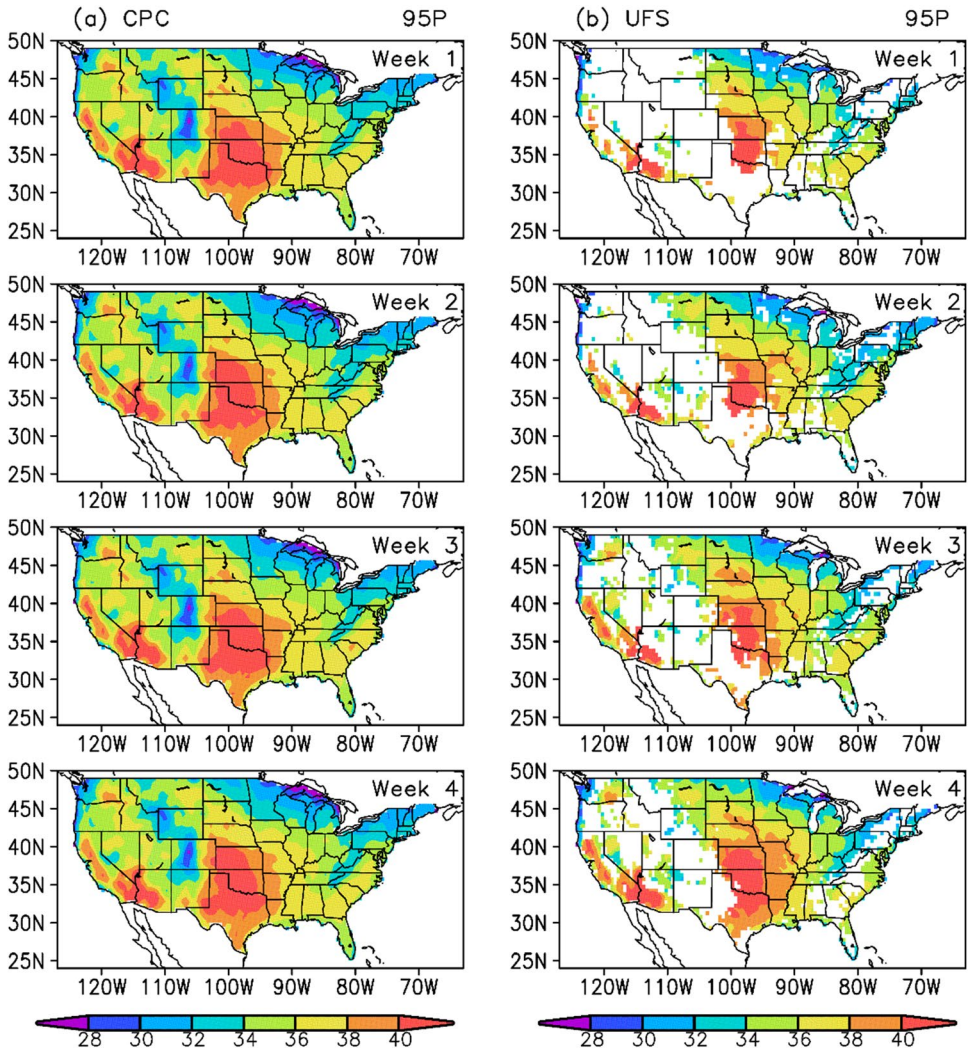

Fig. 5 Weekly composites of maximum temperature per event (°C) above 95P of CPC in **a** CPC observations and **b** UFS forecasts. The first 4 weeks of the forecasts initiated from 1st and 15th of each month during JJAS 2011–2017 are used in the composites. The unshaded white regions over CONUS indicate that the extreme events did not occur at those grid points

and observations are based on the corresponding percentile thresholds of the observation.

4.1 Weekly predictions

The weekly precipitation exceeding the 95P threshold for the first 4 weeks of the forecasts are shown in Fig. 3. The weekly events in the observation (Fig. 3a) have lower values (less than 24 mm day^{-1}) over the western states and higher values over the Midwest and southern states (reaching up to 42 mm day^{-1}). The weekly events have close resemblance to the seasonal composites (Fig. 2a) but do not show extreme events over parts of the West and Texas during certain weeks. The weekly composites in the model forecasts (Fig. 3b) show the extreme events as the lead of the predictions increases. For each of the 4 weeks, the model's performance is somewhat similar and shows higher values in the eastern part and lower values in the western part of CONUS compared to the observations. The difference between the forecasts and observations remains relatively the same from week to week. To obtain a more precise picture of the prediction of the same events as a function of the lead time, week 3 events in observation (Fig. 4a) are compared with the forecasts at lead 1 and 3 weeks (Fig. 4b, c), using the forecasts initiated from 15th and 1st days of month, respectively. Similarly, the week 4 events in observations (Fig. 4d) are compared with forecasts with lead 2 and 4 weeks (Fig. 4e, f). These comparisons are limited because of the design of the forecasts. Although the forecasts have the same spatial structure but with higher values in the eastern part and lower values in the western part of CONUS compared to the observations, there is no large difference in the magnitude of the forecasts at different leads.

The weekly events in maximum temperature above the 95P threshold are shown in Fig. 5 for observation and model forecasts. In the observation (Fig. 5a), the weekly composites are similar to the seasonal composites (Fig. 2c) but with slightly different structure in each week. The maximum temperature is above 40 °C over Texas and neighboring states and Southwest while some northern and western states are

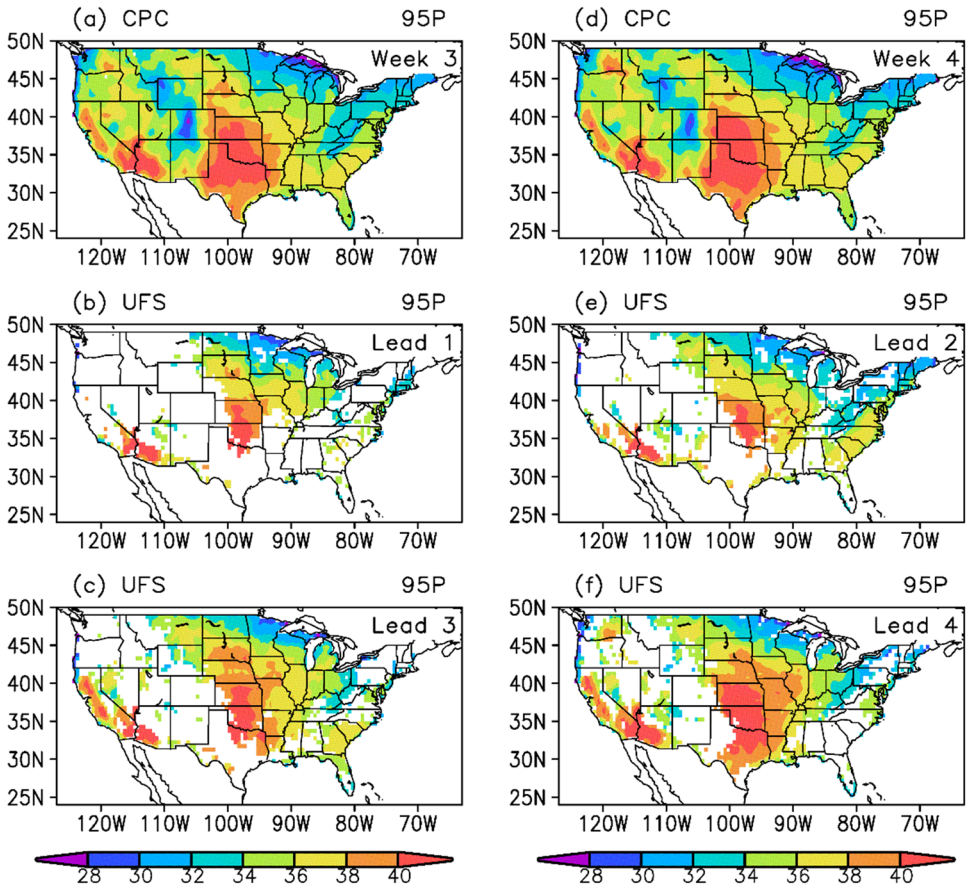

Fig. 6 Weekly composites of maximum 2 m temperature per event (°C) above 95P of CPC in **a** CPC observations for week 3, and corresponding UFS forecasts with **b** lead of 1 week and **c** lead of 3 weeks. Weekly composites of **d** CPC observations for week 4, and corresponding UFS forecasts with **e** lead of 2 week and **f** lead of 4 weeks. The first 4 weeks of the forecasts initiated from 1st and 15th of each month during JJAS 2011–2017 are used in the composites. The unshaded white regions over CONUS indicate that the extreme events did not occur at those grid points

below 34 °C. While the forecasts fail to predict the extreme events over much of the western and southern regions, the magnitudes of the events where they occur are closer to the observed values. Following the procedure used for precipitation, the forecasts of the maximum temperature at leads 1 and 3 weeks are compared with the week 3 observation (Fig. 6a) as well as forecasts at leads 2 and 4 weeks with the week 4 observation (Fig. 6b). The forecasts at different leads do not reveal appreciable differences among them.

For the minimum temperature, the weekly composites in the observations below the 5P threshold (Fig. 7a) are similar to the seasonal composite (Fig. 2e) and cover a large region in the north with temperature below 6 °C while the southern region is above 12 °C. The model is unable to predict the extreme events over some regions in weeks 1–3 but improves in week 4 with predictions closer to the observations over much of the CONUS except for a few states in the West. Similar to the earlier procedure, the week 3 observations below 5P threshold (Fig. 8a) are compared with forecasts at leads 1 and 3 weeks (Fig. 8b, c) showing the model's inability to predict the extreme events over some of western states at 2 weeks lead. However, for the week 4 observation (Fig. 4d), the model improves its coverage from lead 2–4 weeks (Fig. 8e, f). It is difficult to discern any appreciable difference in the magnitude at different leads.

4.2 Forecast error

A quantitative assessment of the forecast skill is now provided by examining the forecast errors and spatial correlations. The root-mean-square (RMS) error in the 95P extreme events in precipitation for the first 4 weeks of the forecasts are presented in Fig. 9. The RMS error was computed as the difference between the weekly precipitation of forecast and observation above the 95P threshold of observation. The errors were averaged for each week using all the forecasts (i.e., those initiated from the 1st and 15th day of each month) over JJAS 2011–2017 at each grid point. In week 1 (day 1 through 7), the errors are relatively large (24–48 mm day^{-1}) over the eastern part of the CONUS and small (less than 24 mm day^{-1}) over the western part (Fig. 9), consistent with the regional differences in the actual magnitudes of the events (Fig. 3). Although the observed extreme events occur at different locations from week to week, the forecast errors have decreased over the eastern CONUS from week 2 to 4. The errors in the precipitation above the 99P threshold also show a similar structure with larger values in the eastern part in week 1 and reduction during weeks 2–4 (Fig. S3). The decrease of error at longer leads can be either due to the small sample size and lack of ensembles or the impact

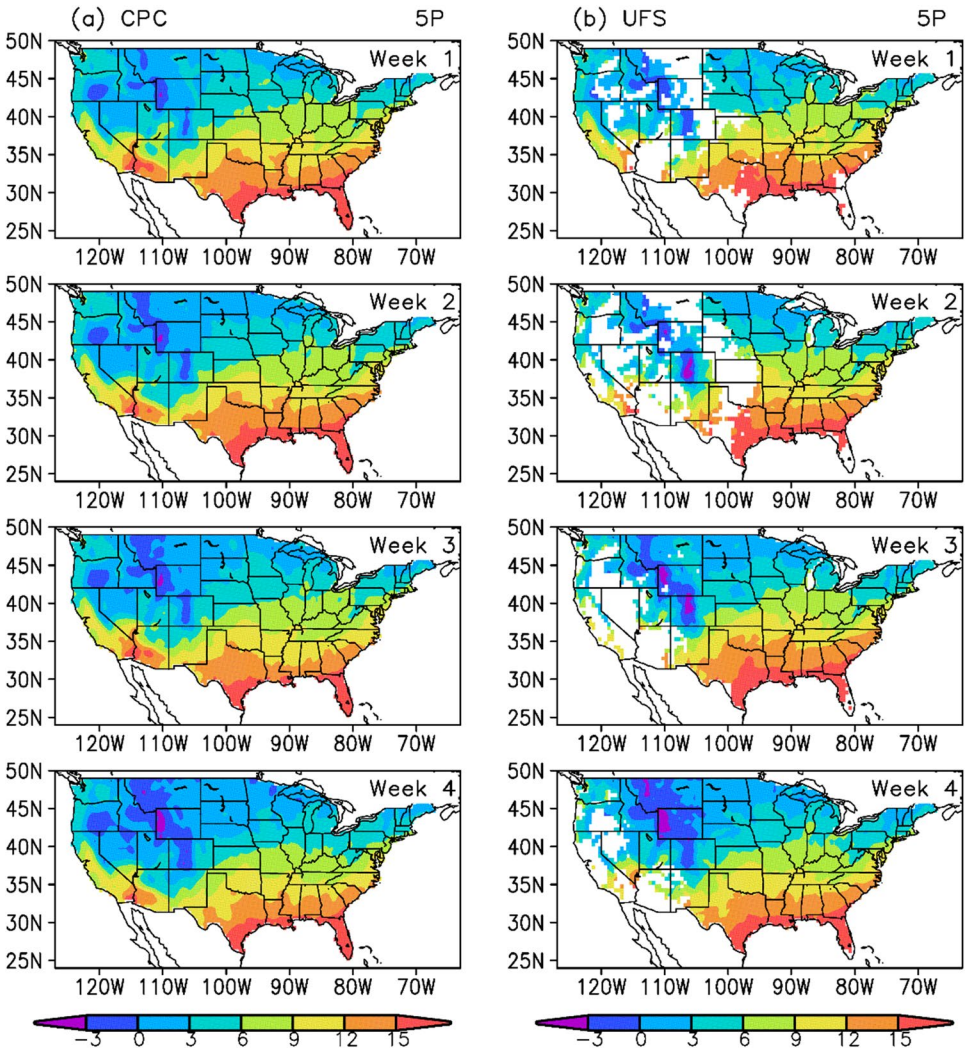

Fig. 7 Weekly composites of minimum temperature per event (°C) below 5P of CPC in **a** CPC observations and **b** UFS forecasts. The first 4 weeks of the forecasts initiated from 1st and 15th of each month during JJAS 2011–2017 are used in the composites. The unshaded white regions over CONUS indicate that the extreme events did not occur at those grid points

of slowly varying sources of predictability. The latter will be explored in Sect. 5.

The weekly RMS errors in the forecast of the maximum temperature above the 95P threshold are shown in Fig. 10a for weeks 1–4. The model fails to predict the extreme events in maximum temperature over a large region in the western part of CONUS. The errors are generally small (below 1.6 °C) during weeks 1–2 but increase during weeks 3–4 with large values (up to 3.2 °C) over the Midwest. The forecast errors in the maximum temperature above the 99P threshold (Fig. S4) show that the model's predictions are confined mainly to the Midwest. The errors are small (mostly about 0.8 °C) during weeks 1–2 and increase (higher than 3.2 °C) during weeks 3–4. The forecast errors of the minimum temperature below the threshold of 5P, shown in Fig. 10b, indicate that the model is able to predict these events over most of the CONUS. The errors are small over most of the CONUS during week 1 but grow during weeks 2–4. The errors reach up to 3.2 °C over the Midwest and Southeast during week 2 and go above 3.2 °C over very large areas during weeks 3–4. The errors in the forecasts of minimum temperature below the 1P threshold (Fig. S4) are small in weeks 1 and 2 but confined to small regions in the eastern and western states. The forecast errors expand during weeks 3 and 4 with large values (up to 3.2 °C) in southern and western states.

4.3 Spatial correlation

A further assessment of the prediction of extreme events is conducted by examining the spatial correlation between observation and model forecasts. Spatial correlation is commonly used to assess the model's ability to predict the observed pattern occurring at a particular time. Spatial patterns are indicative of the inherent dynamics. Since the extreme events may not really evolve with time but may reveal certain spatial pattern related to the inherent dynamics, spatial correlation is a useful measure to assess the model's predictability. The weekly spatial maps of 56 forecasts over CONUS during JJAS 2011–2017 were concatenated

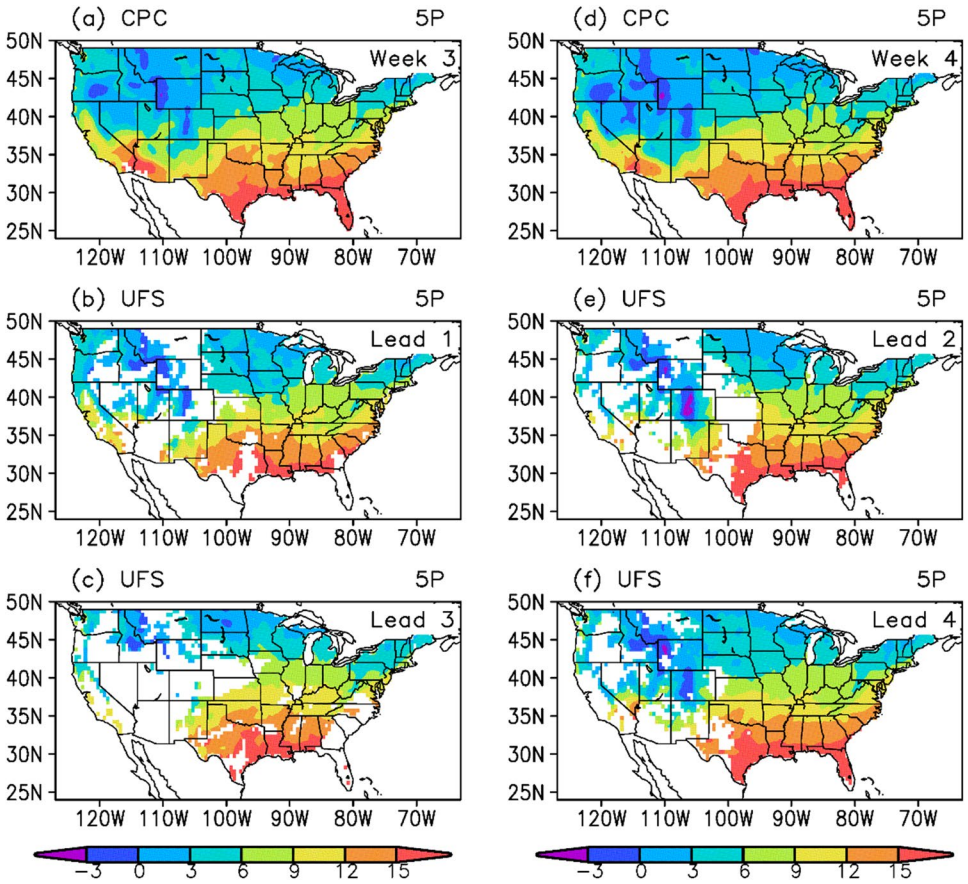

Fig. 8 Weekly composites of minimum 2 m temperature per event (°C) below 5P of CPC in **a** CPC observations for week 3, and corresponding UFS forecasts with **b** lead of 1 week and **c** lead of 3 weeks. Weekly composites of **d** CPC observations for week 4, and corresponding UFS forecasts with **e** lead of 2 week and **f** lead of 4 weeks. The first 4 weeks of the forecasts initiated from 1st and 15th of each month during JJAS 2011–2017 are used in the composites. The unshaded white regions over CONUS indicate that the extreme events did not occur at those grid points

separately for weeks 1–4 of the forecasts. After constructing similar series of maps of the observations for the corresponding times, the spatial correlation between forecasts and observations were computed for weeks 1–4 of the forecast. The spatial correlations were computed separately for the number of extreme events and the magnitude of the events for each variable and for different percentile thresholds. The computation of the correlations involves only those events that the model generates in the particular threshold level.

The spatial correlations of precipitation above the 95P threshold are shown in Fig. 11a for the number of events and the magnitude of the event. The precipitation per event is calculated by dividing the sum of the extreme values by the number of events, separately for forecasts and observation. The number of events in each case may differ between forecasts and observation at any grid point. The spatial correlation takes into account only those grid points where the extreme events occur in both the forecasts and observations The correlation of the number of events starts with 0.25 in week 1 and reduces to below 0.1 in the subsequent weeks. The precipitation per event has higher correlation, although moderate, starting near 0.5 in week 1 and remaining at about 0.4 in weeks 2–4. The correlations of the precipitation above the 99P threshold (Fig. S5a) show that model has almost no correlation in the number of events but has moderate correlation (0.5–0.6) in the magnitude whenever it can generate such extreme events. The correlation of the maximum temperature above the 95P threshold (Fig. 11b) shows contrasting behavior between the number of events and the magnitude of the events. The correlation of the number of events is low (0.2–0.4) while the temperature per event has a correlation of about 0.9 during weeks 1–4. This behavior reflects the fact that the model is able to better predict the values of the extreme events in maximum temperature whenever it can generate such events, consistent with the earlier discussions of the weekly composites (Fig. 5) and forecast errors (Fig. 10). The correlations of the maximum temperature above the 99P threshold (Fig. S5b) are similar to those of the 95P events but with slightly lower value for the number of events. The correlations of the minimum temperature below the 5P threshold (Fig. 11c) reveal slightly better prediction by the model with correlation of the number events in the moderate range of 0.4–0.5 while the correlation of the temperature per event is higher than 0.9 for all the 4 weeks. This behavior implies that the model is able to generate the number of extreme events in the minimum temperature better than those in the maximum temperature at the 95P level. The correlations of the minimum temperature below the 1P threshold (Fig. S5c) also have very high value (above 0.9)

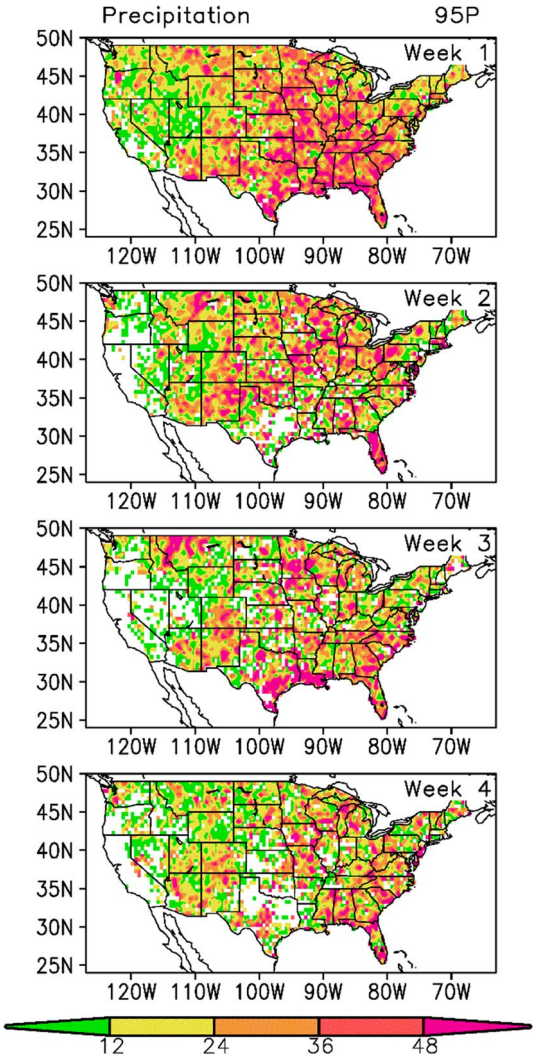

Fig. 9 RMS errors of UFS forecasts in precipitation (mm day^{-1}) above 95P of observation for the first 4 weeks of the forecasts. The RMS errors were computed using all the forecasts initiated from 1st and 15th of each month during JJAS 2011–2017. The unshaded white regions over CONUS indicate that the extreme events did not occur at those grid points

in the temperature per event but the number of events has a lower value (0.2–0.3).

Although the spatial correlation of the number of events is low, the model may still be generating the extreme events in locations other than in the observations. To examine this possibility, the total number of grid points where the extreme events occur was calculated for all the days of weeks 1–4 predictions. The ratio of the number of grid points in the forecasts to that in the observations is shown in Fig. S6. The number of events in the model precipitation is about 1.5–2 times higher than in the observation for 95P and about 2–3 times for 99P (Fig. S6a). However, the ratio is in the range of 0.2–0.8 for the maximum temperature (Fig. S6b) and around 0.2 for the minimum temperature (Fig. S6c). These results suggest that the model is able to generate more extreme events in precipitation but with less accuracy in the location while the events in the temperature are quite less but with higher accuracy in the location, when compared to observations.

5 Relation with leading modes of variability

In a recent study (Krishnamurthy et al. 2021), the predictability of a previous version of the UFS was investigated at subseasonal time scale in terms of three leading modes of variability. For this purpose, the leading modes of variability during the boreal summer (JJAS) were obtained by applying multi-channel singular spectrum analysis (Ghil et al. 2002) on the daily anomalies of 850 hPa horizontal wind (zonal and meridional) over a domain consisting of CONUS and adjoining ocean and land regions. This analysis yielded three leading space-time modes, according to the variance explained. These three modes were identified to be related to El Niño-Southern Oscillation (ENSO), intraseasonal oscillation (ISO) with a period of 50 days and warming trend of the oceans. The principal components (PCs) of the reconstructed components (RCs) of these three leading modes of the 850 hPa horizontal wind were projected on other fields in both observations and model forecasts. The details of the procedure and the analysis of the modes are provided by Krishnamurthy et al. (2021).

The MSSA of the horizontal wind by Krishnamurthy et al. (2021) was performed for the period 1979–2017, and the three leading modes were determined to be statistically significant at 5%. Therefore, the segment of these modes, including the warming trend. for the period 2011–2017 are parts of the statistically significant modes of the longer period. The RCs of the 850 hPa horizontal wind corresponding to the ENSO, ISO and warming trend modes obtained by Krishnamurthy et al. (2021) are projected on the daily anomalies of the observed and model forecast fields used in the present study. The anomalies are computed with respect to the corresponding climatologies in observation and forecasts. These projections yield the daily RCs corresponding to ENSO, ISO and warming trend in the daily anomalies of precipitation, daily maximum and minimum 2 m temperatures for the period JJAS 2011–2017 in observations and model forecasts. The composites of the RCs of the precipitation in the three leading modes of observations and model forecasts were constructed on the basis of the observed daily total precipitation exceeding the 95P threshold (shown in Fig. 1a) for the period JJAS 2011–2017. These composites are constructed exactly the same way as the seasonal composites presented in Fig. 2a and b. Since the RCs of the modes correspond to anomalies, the composites will indicate whether the modes have enhancing or diminishing influence

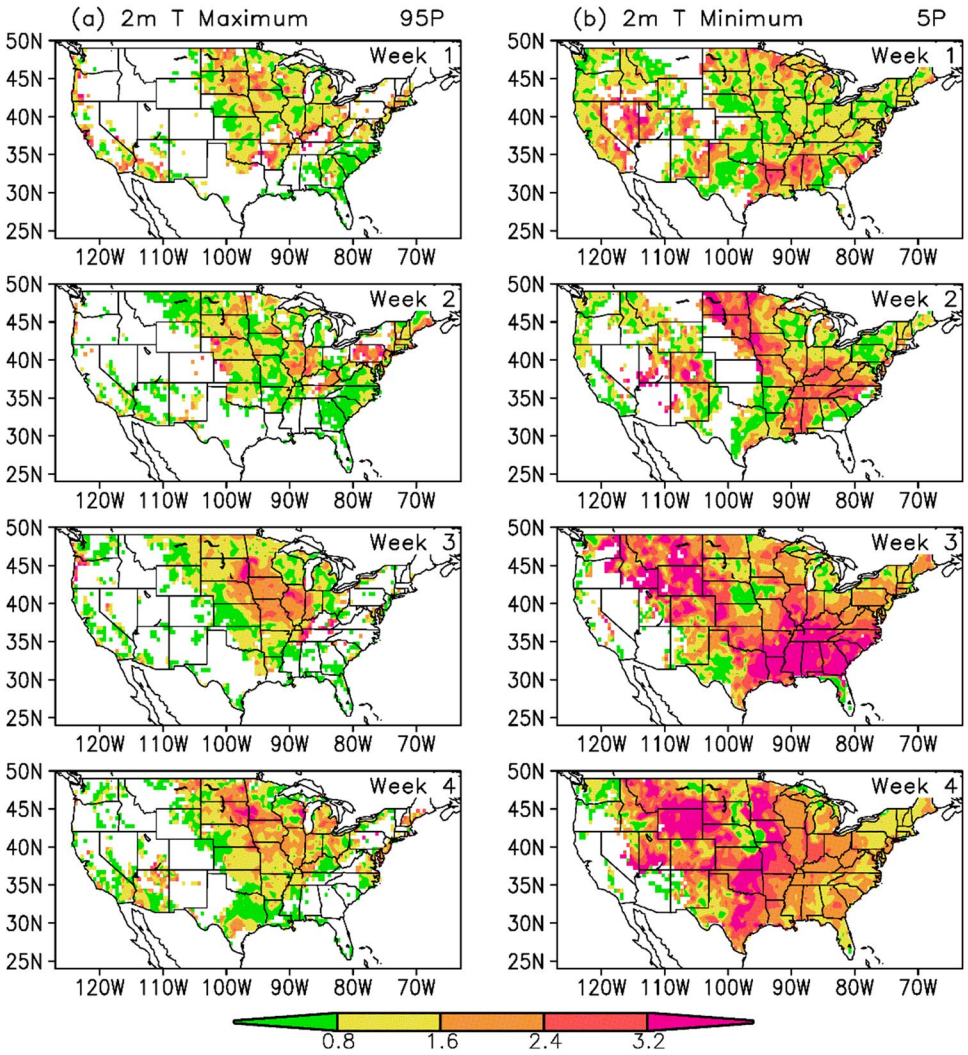

Fig. 10 **a** RMS errors of UFS forecasts in maximum 2 m temperature (°C) above 95P of observation and **b** RMS errors in minimum 2 m temperature (°C) below 5P of observation for the first 4 weeks of the forecasts. The RMS errors were computed using all the forecasts initiated from 1st and 15th of each month during JJAS 2011–2017. The unshaded white regions over CONUS indicate that the extreme events did not occur at those grid points

in the generation of the extreme events. Similar mode composites were constructed for the extreme events in maximum temperature above 95P threshold and in the minimum temperature below 5P threshold.

The composites of precipitation and temperature in the ENSO mode are shown in Fig. 12. In the observed precipitation (Fig. 12a), positive anomalies are present over almost the entire CONUS with higher values in the southern, northeastern and west coast states. The model forecasts (Fig. 12b) also have positive anomalies over the CONUS but the highest values are over a limited region compared to the observation. The ENSO composite of the maximum temperature in the observation (Fig. 12c) also has positive anomalies over the entire CONUS but shows the highest values over Texas and neighboring states similar to the composite in Fig. 2c. The model composite of the maximum temperature (Fig. 12d) also has positive anomalies over the eastern part with the maximum region shifted to the north while missing large regions in the West. The ENSO composite of the minimum temperature (Fig. 12e) consists of negative anomalies over the CONUS except for parts of the Northeast and Florida. Some regions in the Midwest and West show the strongest anomalies. The composite of the model forecasts (Fig. 12f) has strong negative anomalies in the southeastern and western states while positive anomalies are also seen in the central part of CONUS.

The composites of the ISO mode in precipitation and temperature are shown in Fig. 13. The composite of observed precipitation (Fig. 13a) has positive anomalies over most of the CONUS and weak negative anomalies over the southern coastal states. The strongest positive anomalies in the central part of Midwest and East coincide with the high positive values seen in the composite of Fig. 2a. The model forecast also has positive anomalies over the CONUS (Fig. 13b) but the strongest anomalies are spread out in the eastern part. The ISO composite of maximum temperature (Fig. 13c) has weak positive and negative anomalies over most of the CONUS while the composite of forecasts (Fig. 13d) also shows weak anomalies but with a different spatial structure. In the ISO composite of the minimum temperature of

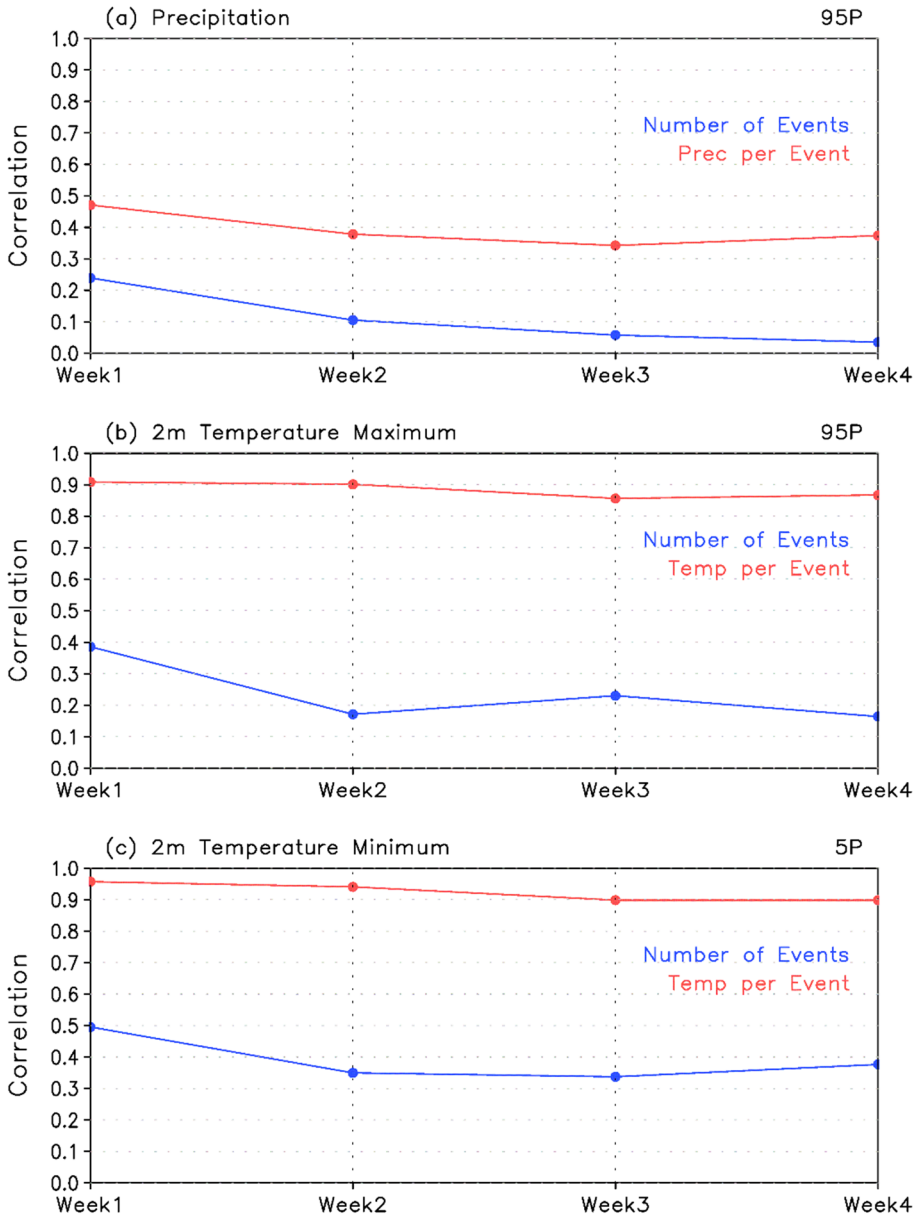

Fig. 11 Spatial correlation between forecasts and observations of **a** number of events (blue) and precipitation per event (red) in precipitation above 95P, **b** number of events (blue) and maximum 2 m temperature per event (red) above 95P and **c** number of events (blue) and minimum 2 m temperature per event (red) below 5P. The correlations were computed using all the forecasts initiated from 1st and 15th of each month during JJAS 2011–2017

observations (Fig. 13e), weak to moderate negative anomalies are present over much of the CONUS and weak positive anomalies over the Southeast and Southwest. The ISO composite of the model forecasts (Fig. 13f) closely resembles the observed composite.

The composites of the warming trend mode are shown in Fig. 14 for precipitation and temperature. The trend composite of the precipitation consists of strong positive anomalies over a large area to the east of 105° W and weaker negative anomalies in the West in both the observation (Fig. 14a) and the forecasts (Fig. 14b). The observations also show negative anomalies in the southeastern region. The strong positive anomalies in the trend mode have good correspondence with the composites of precipitation in Fig. 2a and b. The trend composite of the maximum temperature in the observation (Fig. 14c) shows weak negative anomalies over most of the CONUS with positive anomalies over small regions in the Southeast and Northwest. The composite of the forecasts (Fig. 14d) is close to the observed composite although with missing events over the West. For the minimum temperature, the trend composite in the observations (Fig. 14e) has positive anomalies over most of the CONUS with stronger values in the northern region while the composite of the forecasts (Fig. 14f) shows a large region in the northern states with moderate negative anomalies.

The composites of the three leading modes of variability reveal clear signatures of their influence on the generation and prediction of the extreme events. For the precipitation, all the three modes have enhancing influence over a large part of the CONUS. However, the ISO and the trend

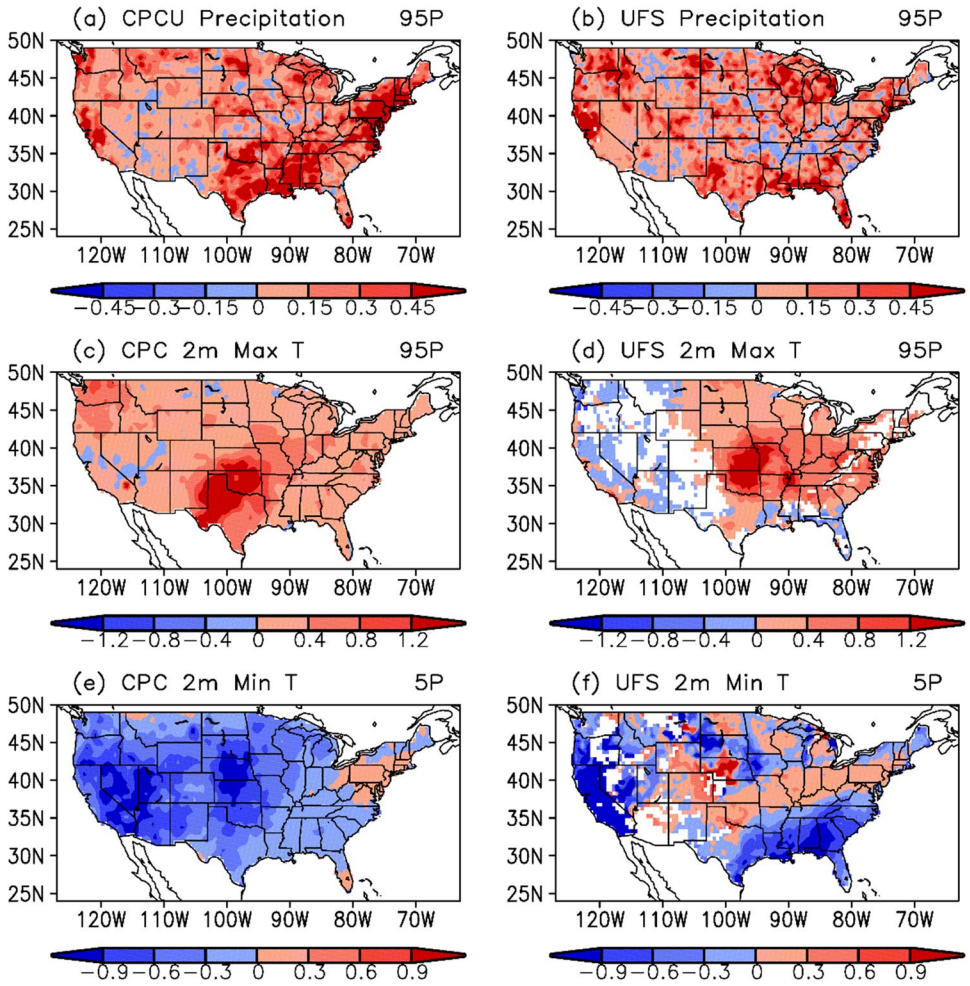

Fig. 12 Composites of ENSO mode of precipitation (mm day^{-1}) in **a** CPCU observation and **b** UFS forecasts based on 95P of CPCU precipitation. Composites of ENSO modes of maximum 2 m temperature (°C) in **c** CPC observation and **d** UFS forecasts based on 95P of CPC maximum temperature. Composites of ENSO modes of minimum 2 m temperature (°C) in **e** CPC observation and **f** UFS forecasts based on 5P of CPC minimum temperature. The composites were computed using all the forecasts initiated from 1st and 15th of each month during JJAS 2011–2017. The composites are averages over the entire period. The unshaded white regions over CONUS indicate that the extreme events did not occur at those grid points

modes are stronger over the central part of the CONUS. The extreme events in the maximum temperature seem to be positively influenced mostly by the ENSO mode, especially over Texas and neighboring states. While the ISO mode has weak mixed influence, the trend mode has moderate negative influence on the maximum temperature. The extreme events in the minimum temperature are enhanced by the negative anomalies associated with the ENSO and ISO modes while diminished by the positive anomalies of the trend mode. The model is able to capture the observed influence of the leading modes to a large extent.

6 Summary and conclusions

This study has examined the predictability of extreme events in the retrospective forecasts of the UFS Coupled Model Prototype 5 during the boreal summer of 2011–2017. The retrospective forecasts of the UFS, generated by the NCEP, are one-month long deterministic predictions from 56 initial conditions (two per month) during the seven boreal summer seasons (JJAS). The extreme events in precipitation, daily maximum 2 m temperature and daily minimum 2 m temperature over the CONUS were examined in both observations and model forecasts. With an emphasis on subseasonal time scale, the performance of the model in predicting the observed weekly composites of extreme events was assessed for weeks 1–4 of the forecast. The influence of the leading modes of variability, identified as related to ENSO, ISO and warming trend, on the generation and predictability of the extreme events was also studied.

The most commonly used criterion based on quantiles was adopted to identify the extreme events in this study. All the analyses were carried out for extreme events in precipitation and daily maximum temperature exceeding the 95th percentile and for events in daily minimum temperature below the 5th percentile. Additionally, some of the analyses were extended to events beyond 99th percentile and 1st percentile accordingly. The observed extreme events show a wide range of values in precipitation and temperature over the CONUS during the boreal summer. The precipitation events have lower magnitude over the western part (< 24 mm day^{-1}) while the central region shows the highest values (> 36 mm day^{-1}). The model forecasts capture the spatial pattern of

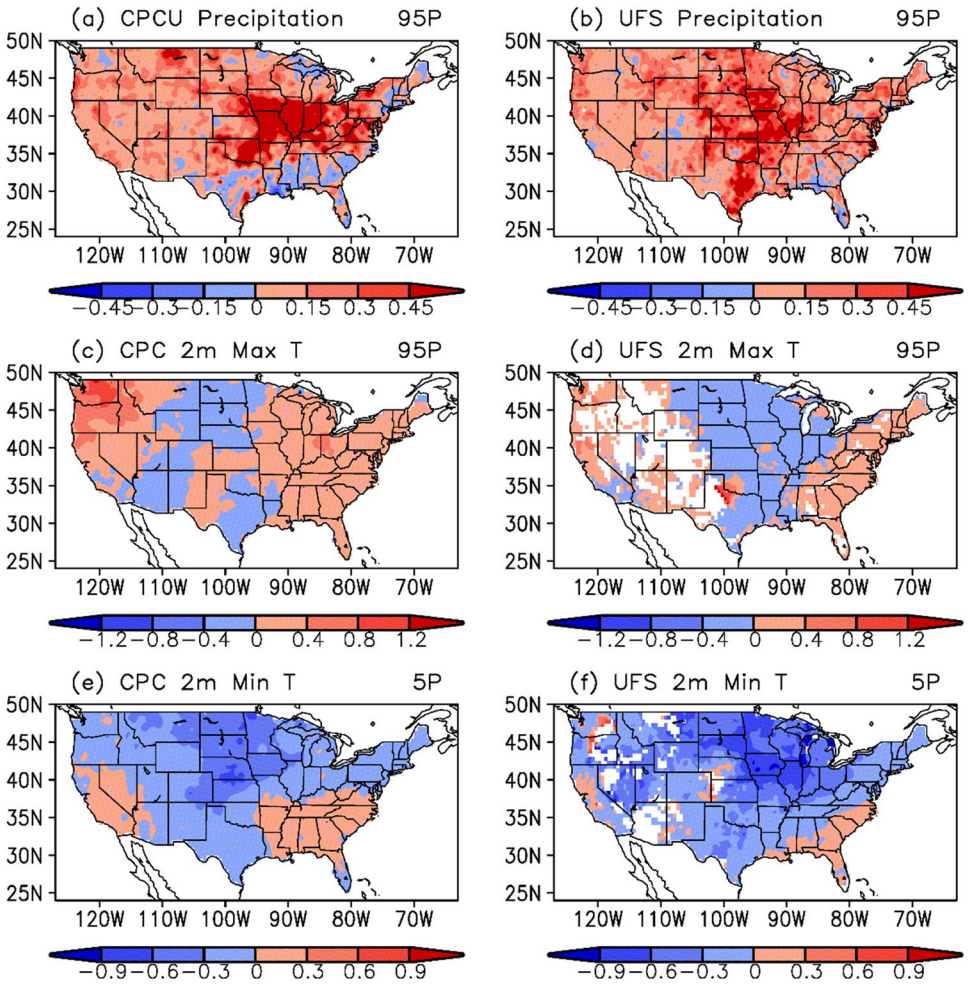

Fig. 13 Composites of ISO mode of precipitation (mm day^{-1}) in **a** CPCU observation and **b** UFS forecasts based on 95P of CPCU precipitation. Composites of ISO mode of maximum 2 m temperature (°C) in **c** CPC observation and **d** UFS forecasts based on 95P of CPC maximum temperature. Composites of ISO mode of minimum 2 m temperature (°C) in **e** CPC observation and **f** UFS forecasts based on 5P of CPC minimum temperature. The composites were computed using all the forecasts initiated from 1st and 15th of each month during JJAS 2011–2017. The composites are averages over the entire period. The unshaded white regions over CONUS indicate that the extreme events did not occur at those grid points

precipitation reasonably well although with slightly higher values. The observed maximum temperature is in range of 28–40 °C with highest values (> 38 °C) over some southern and southwestern states. Although the forecasts are close to the observed values, the model fails to generate the extreme events over a large region in the West. The daily minimum temperature in the observation covers a large northern region with lower values (< 6 °C) whereas the southern states have the highest values (> 15 °C). The model forecasts capture the observed pattern with slightly higher values but miss several areas in the western states.

The weekly extreme events follow the same patterns as the seasonal events in both the observations and model forecasts. The model predictions of the events in precipitation are larger than observation over the CONUS with errors above 24 mm day^{-1} in the eastern part and do not change appreciably from week 1 to 4. The magnitude of the errors is somewhat proportional to the value of the extreme events. The spatial correlation between observation and model forecasts is almost negligible while the precipitation per event has moderate correlation. The model generates higher number of extreme events in precipitation compared to observations but with less accuracy in their locations. These results indicate that the model is able to capture the magnitude and spatial pattern reasonably well over large regions, but the prediction at very local level (or grid point level) is far from accurate. The model's prediction of the daily maximum temperature varies widely from week 1 to 4 in its ability to generate the extreme events although the magnitude is close to the observation where it succeeds. Although the spatial correlation of the number of events between forecasts and observation is low (around 0.2), the correlation of the temperature per event is very high (around 0.9) for all the weeks. This implies that there is less local variation in the magnitude of the temperature events compared to the precipitation as well as that the model is more accurate in predicting the temperature events whenever and wherever it can generate them. The behavior of the daily minimum temperature is similar to the maximum temperature but with minor differences. The model is able to predict the minimum temperature over a larger region but the errors grow from week 1 to 4. The

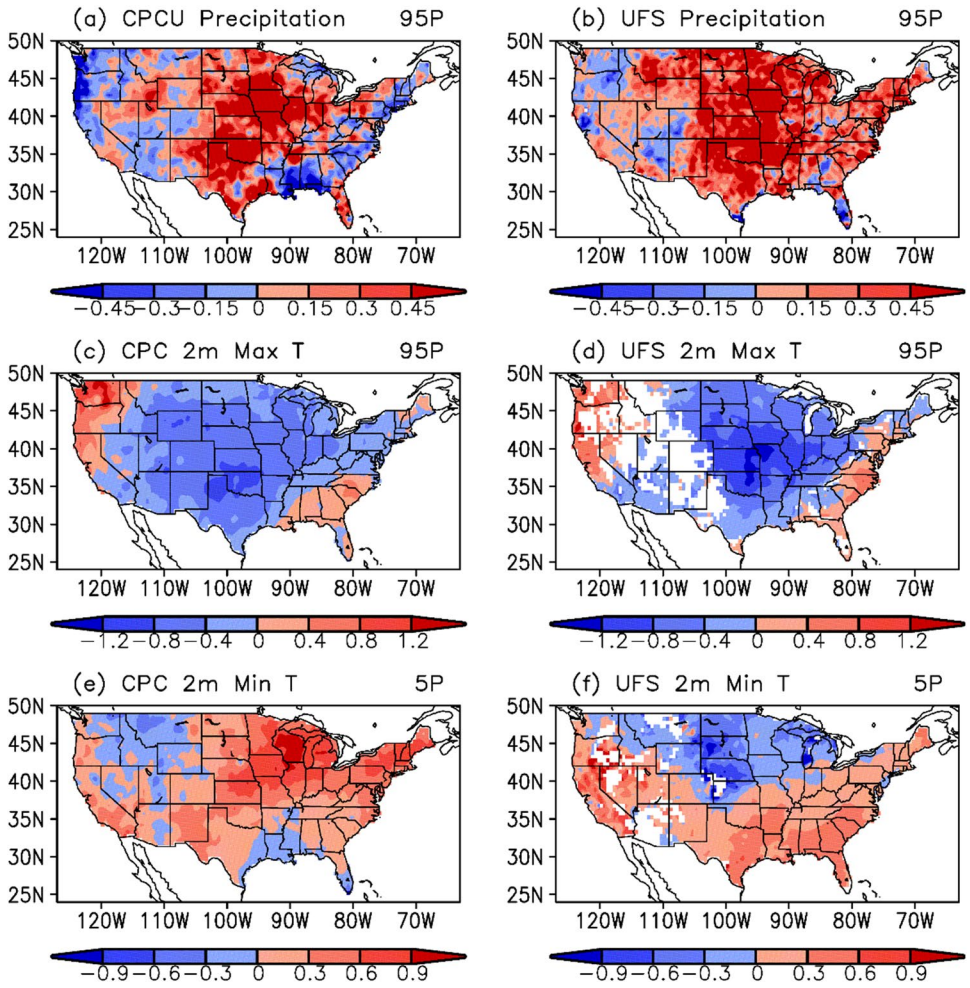

Fig. 14 Composites of warming trend mode of precipitation (mm day^{-1}) in **a** CPCU observation and **b** UFS forecasts based on 95P of CPCU precipitation. Composites of warming trend mode of maximum 2 m temperature (°C) in **c** CPC observation and **d** UFS forecasts based on 95P of CPC maximum temperature. Composites of warming trend mode of minimum 2 m temperature (°C) in **e** CPC observation and **f** UFS forecasts based on 5P of CPC minimum temperature. The composites were computed using all the forecasts initiated from 1st and 15th of each month during JJAS 2011–2017. The composites are averages over the entire period. The unshaded white regions over CONUS indicate that the extreme events did not occur at those grid points

spatial correlation of the number of events in the minimum temperature is of moderate value (around 0.4) while the correlation of the temperature per event is very high (above 0.9). These results suggest that a higher initialization frequency can improve the model's ability to generate the extreme events.

The leading modes of variability over CONUS and adjoining oceanic and land regions, obtained through MSSA, are related to ENSO, ISO and warming trend. The influence of these modes was studied by examining the seasonal composites of each mode based on the extreme events in each field. Since the space-time structures of the leading modes are coherent, their association with the extreme events show clear signatures. While all the three modes have enhancing influence over a large part of the CONUS in the precipitation events, the ISO and the trend have the strongest influence over the central region. For the maximum temperature, the extreme events have positive enhancement mostly by the ENSO mode whereas the ISO mode has weak mixed influence and the trend mode has moderate negative influence. The ENSO and ISO modes enhance the extreme events in the minimum temperature while the trend mode has diminishing influence. The focus of the study has been on the impact of large-scale modes of climate variability on the extremes of atmospheric weather. In addition to these environmental conditions, there are other local influences, such as land-atmosphere interactions (Dirmeyer 2000; Zhang et al. 2008; Mei and Wang 2012), convective processes (Gao et al. 2017; Prein et al. 2017) and small-scale circulations (Higgins et al. 1997; Angel et al. 2015; Abatzoglou 2016), that contribute to extreme events and need to be addressed when evaluating the forecast skill of a prediction system.

Supplementary Information The online version contains supplementary material available at https://doi.org/10.1007/s00382-021-06120-0.

Acknowledgements This work was supported by the National Oceanic and Atmospheric Administration (grant NA18NWS4680069) and by the Unified Forecast System Research to Operation (UFS R2O) Project which is jointly funded by NOAA's Office of Science and Technology Integration (OSTI) of National Weather Service (NWS) and Weather Program Office (WPO), [Joint Technology Transfer Initiative (JTTI)] of the Office of Oceanic and Atmospheric Research (OAR) through the NOAA grant NA19NES4320002 (Cooperative Institute for Satellite Earth System Studies-CISESS). Data used in this study are publicly

available at https://registry.opendata.aws/noaa-ufs-s2s/. The authors thank three anonymous reviewers for helpful comments.

Declarations

Conflict of interest The authors declare no conflict of interest.

References

Abatzoglou TJ (2016) Contributions of cutoff lows to precipitation across the United States. J Appl Meteorol Climatol 55:893–899

Adcroft A et al (2019) The GFDL Global Ocean and Sea Ice Model OM40) model description and simulations features. J Adv Model Earth Syst 11:3167–3211

Angel L et al (2015) Climatology of daily precipitation and extreme precipitation events in the Northeastern United States. J Hydrometeorol 15:2537–2557

Barlow M et al (2019) North American extreme precipitation events and related large-scale meteorological patterns: a review of statistical methods dynamics modeling and trends. Clim Dyn 53:6835–6875

Clark RT, Brown SJ, Murphy JM (2006) Modeling Northern Hemisphere summer heat extreme changes and their uncertainties using a physics ensemble of climate sensitivity experiments. J Clim 19:4418–4435

Dee DP et al (2011) The ERA-Interim reanalysis: configuration and performance of the data assimilation system. Q J R Meteorol Soc 137:553–597

Dirmeyer PA (2000) Using global soil wetness dataset to improve seasonal climate simulation. J Clim 13:2900–2922

Gao Y, Leung LR, Zhao C, Hagos S (2017) Sensitivity of US summer precipitation to model resolution and convective parameterizations across gray zone resolutions. J Geophys Res Atmos 122:2714–2733

Ghil M et al (2002) Advanced spectral methods for climatic time series. Rev Geophys 40(1):1003. https://doi.org/10.1029/2000RG000092

Grotjahn R et al (2016) North American extreme temperature events and related large scale meteorological patterns: a review of statistical methods dynamics modeling and trends. Clim Dyn 46:1151–1184

Higgins WY, Yao Y, Yarosh ES, Janowiak JE, Mo KC (1997) Influence of the Great Plains low-level jet on summertime precipitation and moisture transport over the central United States. J Clim 10:481–507

Huang H et al (2021) Sources of subseasonal-to-seasonal predictability of atmospheric rivers and precipitation in the western United States. J Geophys Res Atmos 126:e2020JD034053. https://doi.org/10.1029/2020JD034053

Jones C (2000) Occurrence of extreme precipitation events in California and relationship with the Madden-Julian Oscillation. J Clim 13:3576–3587

Jones C, Gottschalck J, Carvalho LMV, Higgins WR (2011) Influence of the Madden–Julian oscillation on forecasts of extreme precipitation in the contiguous United States. Mon Weather Rev 139:332–350

Klotzbach PJ, Oliver ECJ, Leeper RD, Schreck CJ (2016) The relationship between the Madden–Julian Oscillation (MJO) and Southeastern New England snowfall. Mon Weather Rev 144:1355–1362

Koster RD et al (2004) Regions of strong coupling between soil moisture and precipitation. Science 305:1138–1140

Krishnamurthy V et al (2021) Sources of subseasonal predictability over CONUS during boreal summer. J Clim 34:3273–3294

Lin H, Mo R, Vitart F, Stan C (2019) Eastern Canada flooding 2017 and its subseasonal predictions. Atmos Ocean 57:195–207

Mei R, Wang G (2012) Summer land-atmosphere coupling in the United States: comparison among observations reanalysis data and numerical models. J Hydrometeorol 13:1010–1022

Prein AF, Rassmussen RM, Ikeda K, Liu C, Clark MP, Holland GJ (2017) The future intensification of hourly precipitation extremes. Nat Clim Change 7:48–52

Seneviratne SI et al (2012) Changes in climate extremes and their impacts on the natural physical environment. In: Field CB, V Barros V, Stocker TF, Qin D, Dokken DJ, Ebi KL, Mastrandrea MD, Mach KJ, Plattner G-K, Allen SK, Tignor M, Midgley PM (eds) Managing the risks of extreme events and disasters to advance climate change adaptation. A special report of working groups I and II of the intergovernmental panel on climate change (IPCC). Cambridge University Press, Cambridge, pp 109–230

Singh D, Tsiang M, Rajaratnam B, Diffenbaugh NS (2013) Precipitation extremes over the continental United States in a transient high-resolution ensemble climate model experiment. J Geophys Res Atmos 118:7063–7086. https://doi.org/10.1002/jgrd.50543

Srivastava A, Grotjahn R, Ullrich PA (2020) Evaluation of historical CMIP6 model simulations of extreme precipitation over contiguous US regions. Weather Clim Extremes 29:100268. https://doi.org/10.1016/j.wace.2020.100268

Stan C, Lin H (2019) Introduction to the special issue of the Year of Tropics-Midlatitude Interactions and teleconnections (YTMIT). Atmos Ocean 57:157–160. https://doi.org/10.1080/20507828.2019.1653032

Stan C, Straus DM, Frederiksen JS, Lin H, Maloney ED, Schumacher C (2017) Review of tropical-extratropical teleconnections on intraseasonal time scales. Rev Geophys 55:902–937. https://doi.org/10.1002/2016RG000538

Vecchi GA, Bond NA (2004) The Madden-Julian Oscillation (MJO) and the northern high latitude wintertime surface air temperatures. Geophys Res Lett 31:L04104. https://doi.org/10.1029/2003GL018645

Vitart F, Robertson AW (2018) The sub-seasonal to seasonal prediction project (S2S) and the prediction of extreme events. npj Clim Atmos Sci 1:3. https://doi.org/10.1038/s41612-018-0013-0

Vitart F et al (2016) The subseasonal to seasonal (S2S) prediction project database. Bull Am Meteorol Soc 98:63–173

Xie P, Chen M, Shi W (2010) CPC unified gauge-based analysis of global daily precipitation. Preprints 24th Conference on Hydrology Atlanta GA American Meteorological Society https://ams.confex.com/ams/90annual/techprogram/paper_163676.htm

Zhang J, Wang WC, Leung LR (2008) Contribution of land-atmosphere coupling to summer climate variability over the contiguous United States. J Geophys Res Atmos 113:D22109. https://doi.org/10.1029/2008JD010136

Zhou S, L'Heureux M, Weaver S, Kumar A (2012) A composite study of the MJO influence on the surface air temperature and precipitation over the Continental United States. Clim Dyn 38:1459–1471

Zhu X, Stan C (2015) Projection of summer precipitation over the southeastern United States in the superparameterized CCSM4. J Clim 28:8052–8066